MEMOIRS OF THE FACULTY OF ENGINEERING
FUKUI UNIVERSITY
VOL. 34 No. 1 1986

Phase-Plane Analyses of Parametrically- and Self-Excited Mechanical Systems

Sumio YANO*

(Received Feb. 28, 1986)

In order to investigate the behaviors of parametrically and self-excited mechanical systems, graphically analytic methods in the phase plane are proposed. Unstable phenomena like parametric and self-excited vibrations happen to appear in rotating machinery with a crack, a rub, the looseness and so on. Such unfavorable vibrations should be detected and predicted as early as possible. In this paper, their characteristics are investigated and a fundamental view for describing and analyzing nonlinear models is presented.

1. Introduction

Parametric and self-excited vibrations happen to endanger the safe operation of machines and lead to the failure. Parametric vibrations are induced by the periodic variation of system parameters and often occur in rotating machinery and in tube systems carrying a fluid like multi-segment articulated tubes. It is well known that rotors with a crack and the looseness due to bearing-clearance effects, and rubbing rotors against the housing or stationary parts like a jammed or off-centered seal[1] give rise to parametric vibrations and/or self-excited ones. Such unfavorable vibrations should be detected by suitable observers and be predicted in the initial stage of occurrence. Firstly the investigation and the classification of characteristics of such vibrations and consequently the description of mathematical models for interpreting them are necessary.

In the present paper typical characteristics of rotors with a crack, a rub and the looseness are presented. As a first step of

* Dept. of Mechanical Engineering

modeling, nonlinear differential equations of motion for interpreting the occurrence of resonances due to parametric excitation are described and some available methods for numerically solving them are presented.

2. Features of Rotors with a Crack, a Rub and the Looseness

We shall grasp the feature of resonance phenomena of rotors with a crack, a rub and a loose disk through the experimental results done by Bently Nevada Corporation[3]-[6] and Darmstadt Technical University[2].

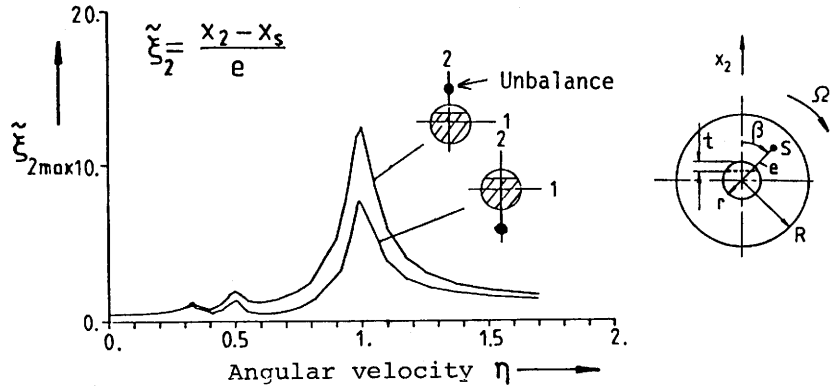

(a) Maximum dynamic deflection in direction 2 for t=0.25r

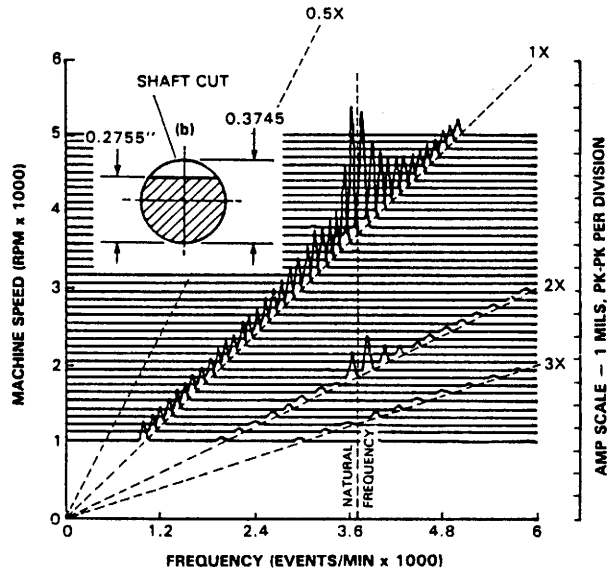

(b) Cascade spectrum of responce versus frequency

Fig.1 Rotors with a crack

Figure 1 shows examples of responce curves[2] and cascade spectra of responce versus frequency[3] for rotors with cracks, though their test rigs are different. Figure (b) shows that superharmonic components of orders 2 and 3 appear in the rotor response (see 2x and 3x)。 Then it is ascertained from Fig.(a) that additional resonances occur at the rotational speeds of 1/2 and 1/3 of main resonance. The occurrence of such resonances will be predicted from nonlinear systems with the periodically varying restoring force of Mathieu type as well as with harmonic external forces due to unbalances.

Figure 2 shows an example of a cascade spectrum of response for a rotor with a light rub and harmonics of the light rub signal. The rub is initiated by brass screws, simulating rubs in seals or at a blade tip and shroud due to insufficient clearances. It is seen from Fig。(a) that subharmonic components of higher orders become dominant in the response over the region of twice the first resonance speed. Figure (b) shows that rub signals themselves complicated frequency components。 Since rub phenomena are concerned with the

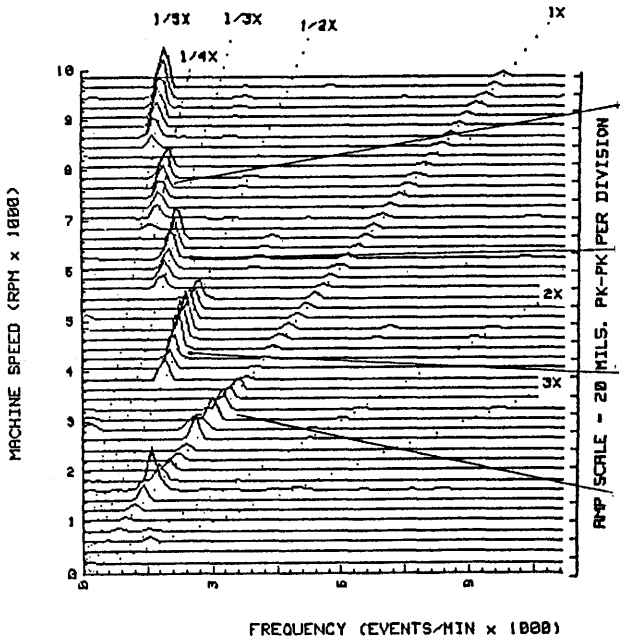

(a) Cascade spectrum of responce versus frequency

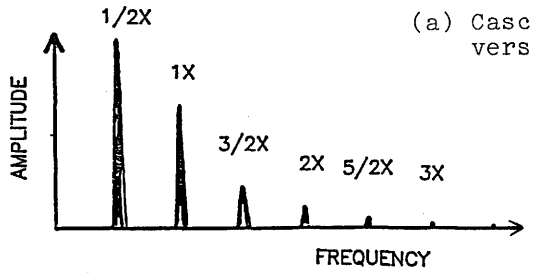

(b) Harmonic components of light rub signals

Fig.2 Rotors with a light rub

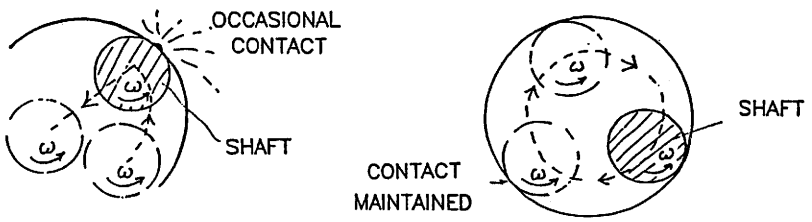

(a) Partial rub (b) Full annular rub

Fig.3 Two types of rubs

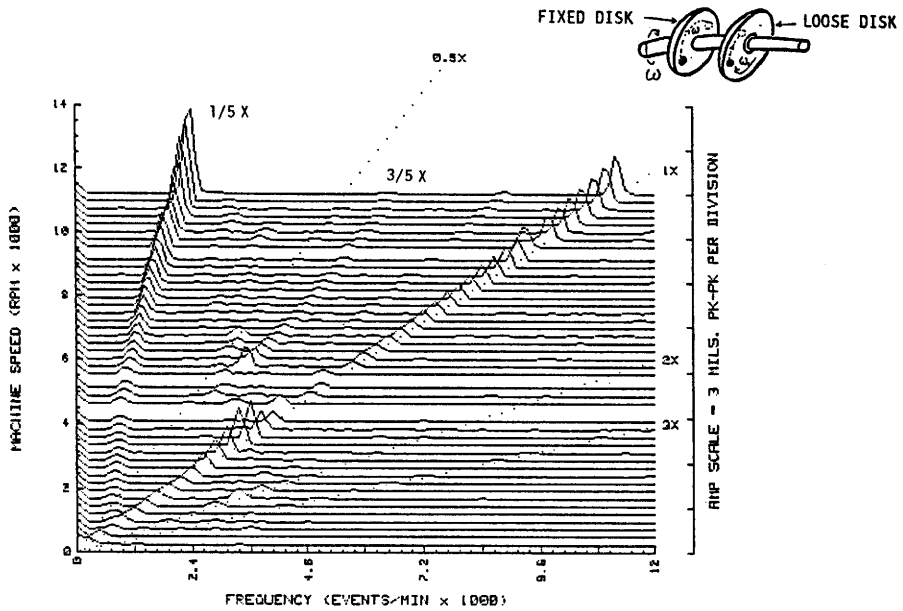

Fig.4 Cascade spectrum of start-up response of rotor with two blade loose disks

occurrence of self-excited vibrations, we need consider them from a viewpoint of the interaction between self-excited vibrations and external excitation due to unbalances. Furthermore if contacts or impacts are periodic, parametric vibrations also arise, so that mathematical models describing their

Table 1 Harmonics of rotor response due to loose disks with blades

Number of blades	Order of harmonics
4	1/4
3	1/6
2	1/5 (start-up) 1/4 (shutdown)

phenomena become complicated. The feature of these phenomena depends on the situation of contacts as shown in Fig.3[5], too.

As an example of a cascade spectrum for rootrs with loose disks, Fig.4[6] shows that of start-up response for the case of two blade loose disks. According to the number of blades, such dominant subharmonic (subsynchronous) components of higher orders as shown in Table 1 appear.

3. Description of Equations of motion

The above-mentioned unstable phenomena belong to vibrational problems of parametrically and/or self-excited systems with external forces and the establishment of available dynamic models are required. As far as the author knows, it seems that nonlinear phenomena of systems subjected to self-excitation and/or parametric one have been not fully studied, though stability analyses by linear models are often performed. So we shall consider dynamic behaviors of such systems due to the interaction between both excitations through nonlinear models governed by the following differential equations where both excitations are idealized typically and plainly. Although those models do not necessarily describe the whole properties of vibrational phenomena mentioned in Chap.2, they might be helpful in predicting the behaviors in the neighborhood of the initiation of instability when the external excitation is not so large.

$$\ddot{y} + g(y)\dot{y} + f(y, \tau) = 0 \ ; \quad \dot{y} = dy/d\tau \qquad (1)$$

where functions g and f are shown in Table 2. As for the parameter μ, there is also the case that μ is a function of η like $\bar{\mu}\eta^2$, which holds for the crank mechanism in wave power machines[7].

Furthermore for some flow-induced vibrations, the following

Table 2 Functions g and f

$g(y)$	Type	$f(y, \tau)$
$-(\delta_0-\delta_2 y^2)$	1	$(1+\sum_{n=1}^{s}\gamma_{n+1}y^n+\mu\cos 2\eta\tau)y$
$\delta_0-\delta_2 y^2+\delta_4 y^4$	2	$(1+\sum_{n=1}^{s}\gamma_{n+1}y^n)(1+\mu\cos 2\eta\tau)y$
$\delta_i>0$ $(i=0, 2, 4)$	3	$(1+\sum_{n=1}^{p}\gamma_{n+1}y^n)(1+\mu\cos 2\eta\tau)y+\sum_{n=p+2}^{s}\gamma_n y^n$

equation whose damping term is described by the sum of self-excitation and parametric excitation might be properer:

$$\ddot{y} + \bar{g}(\dot{y})\bar{f}(\tau)\dot{y} + (1+\sum_{n=1}^{s}\gamma_{n+1}y^{n})y = 0 \qquad (2)$$

where for example,

$\bar{g}(\dot{y})=-\{\delta_0-\delta_2(\dot{y})^2\}$, $\bar{f}(\tau)=1+\mu\cos 2\eta\tau$.

We shall proceed to analyses of system (1), assuming that nonlinear parameters are quite smaller than unity and the system is not entirely dominated by self-excitation. In Chapter 4 graphical methods by phase trajectories are presented and in Chapter 5 an approximate analytical method is shown.

4. Expression of Phase Trajectories

We shall numerically solve differential equations governed by system (1) by means of Runge-Kutta-Gill (RKG) method and grasp their behavior by the phase trajectories. Since system (1) is non-autonomous and its trajectories in the classical plane $y-\dot{y}$ are rotatory with crossing each other, the author proposes the following two methods by more comprehensive trajectories.

4.1 Trajectories in the rotating coordinates

Before this method is explained, we consider the behavior of a solution like $y=A\cos(n\eta\tau/m-\phi)$ (n/m: order of resonance, A: amplitude; ϕ: phase) and its velocity $\dot{y}$ in the phase plane. Then the following relation holds:

$$y^2+(m\dot{y}/n\eta)^2=A^2 \qquad (3)$$

Relation (3) means an elliptical orbit in the plane $y-\dot{y}$ and also a circle of radius A rotating with an angular velocity $n\eta/m$ in the plane $y-(m\dot{y}/n\eta)$. Then its circle can be transformed to be a point in the plane $\xi-\zeta$ rotating with an angular velocity $n\eta/m$ (see Fig.5). Although both A and ϕ are not constant, its movement in the rotating coordinstes will be very slow and the observation of its behavior in this coordinate system will help our understanding when the variation of A and ϕ are fully small or varies far more slowly than $n\eta/m$.

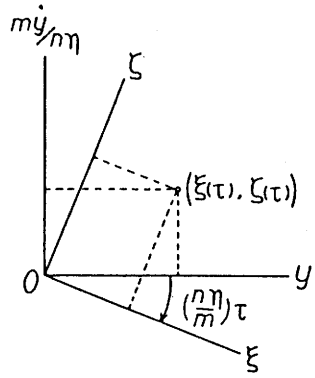

Fig.5 Coordinate system

Since the trajectory expressed in the rotating coordinates is considered to be more convenient, we express such trajectories in the following procedure:

By the formula of variables:

$$y_1 = y\ ,\quad y_2 = m\dot{y}/n\eta \tag{4}$$

system (1) yields the first-order differential equations for numerical integration as follows:

$$\left.\begin{aligned} \dot{y}_1 &= (n\eta/m)y_2\ , \\ \dot{y}_2 &= -g(y_1)y_2 - (m/n\eta)f(y_1, \tau) \end{aligned}\right\} \tag{5}$$

By using the following formula of coordinate transformation:

$$\begin{bmatrix} \xi \\ \zeta \end{bmatrix} = \begin{bmatrix} \cos(n\eta\tau/m) & -\sin(n\eta\tau/m) \\ \sin(n\eta\tau/m) & \cos(n\eta\tau/m) \end{bmatrix} \begin{bmatrix} y_1 \\ y_2 \end{bmatrix} \tag{6}$$

the integrated values y_1 and y_2 at each time are transformed consecutively into values ξ and ζ. Accordingly trajectories in the plane y_1-y_2 are expressed in the plane ξ - ζ.

4.2 Trajectories in the stroboscope phase plane

This method is more convenient for grasping resonance phenomena because it is based on the periodicity. Let the period of vibration be T. The numerical integration of Eq.(6) is likewise performed but the determination of its time increment $\Delta\tau$ is different from that used in Sec.4.1 (for example, $\Delta\tau$=0.1). For this method $\Delta\tau$ is determined by $\pi/(N\eta)$, where N is an integer dividing 2π to sample $2\eta\tau$, that is, satisfying the following relation:

$$2\eta\tau = 2\pi/N \tag{7}$$

where the N should be chosen so that $\Delta\tau$ corresponds to that used in Sec.4.1, for example, such N as 24 is used for $\eta \simeq 1$.

Trajectories in the stroboscope phase plane are drawn by connecting reference points at every period $[y(T), m\dot{y}(T)/n\eta]$, $[y(2T), m\dot{y}(2T)/n\eta]$, ... instead of original points $[y(\tau), m\dot{y}(\tau)/n\eta]$ integrated at each time. This operation corresponds to the Poincaré mapping in mathematics and the reference point corresponds to a fixed point. Concretely every $(2m/n)N$ th original point is plotted for a resonance of order n/m, where m=1, 2, ... and n=1 or 2. Then resonances of order n/m are characterized by $2m$ stable singular points (see Fig.7).

The stroboscope phase plane is denoted by (y)-$(m\dot{y}/n\eta)$ in distinction from the original plane y - $m\dot{y}/n\eta$. When the system nonlinearity is quite small and original trajectories are close to circles, trajectories for resonances of order n/m expressed in the plane (y)-$(m\dot{y}/n\eta)$ are similar to those in the plane (y)-$(\dot{y})$ because the relation $\eta \simeq m/n$ holds. The stroboscope phase plane itself is named by Tondl[8] because the behavior seems to be observed through a stroboscope.

5. Approximate Analytical Method

As a method of approximate analysis, the author uses the averaging method in harmony with the above-mentioned phase-plane analysis from viewpoints shown in Table 3. The assumption of analysis that nonlinear parameters are quite small will correspond to the fact that phase trajectories are close to circles.

Table 3 Phase trajectory and approximate analysis

Viewpoint	Phase trajectory	Approximate analysis
Equation of motion of rotating schaft with asymmetric stiffness: In the fixed coordinates —— periodic coefficients In the rotating coordinates —— constant coefficients	Expression in the rotating coordinates	
The periodicity of system parameters induces vibrations: Pursuit of behaviors at every one period of vibration	Trajectory in the stroboscope phase plane	Analysis by averaging method

Assuming a solution of Eq.(5) as follows:

$$\left.\begin{aligned} y_1 &= \xi\cos(n\eta\tau/m) + \zeta\sin(n\eta\tau/m) + z_1 = A\cos(n\eta\tau/m - \phi) + z_1 \\ y_2 &= -\xi\sin(n\eta\tau/m) + \zeta\cos(n\eta\tau/m) + z_2 = -A\sin(n\eta\tau/m - \phi) + z_2 \end{aligned}\right\} \quad (8)$$

and after a rearrangement the following differential equations are derived:

$$\left.\begin{aligned} \dot{\xi} &= -\dot{z}_1\cos(n\eta\tau/m) + \dot{z}_2\sin(n\eta\tau/m) + (n\eta/m)z_2\cos(n\eta\tau/m) \\ &\quad -(n\eta/m)(y_1 - z_1)\sin(n\eta\tau/m) + g(y_1)\,y_2\sin(n\eta\tau/m) \\ &\quad +(m/n\eta)f(y_1, \tau)\sin(n\eta\tau/m) , \\ \dot{\zeta} &= -\dot{z}_1\sin(n\eta\tau/m) - \dot{z}_2\cos(n\eta\tau/m) + (n\eta/m)z_2\sin(n\eta\tau/m) \\ &\quad +(n\eta/m)(y_1 - z_1)\cos(n\eta\tau/m) - g(y_1)\,y_2\cos(n\eta\tau/m) \\ &\quad -(m/n\eta)f(y_1, \tau)\cos(n\eta\tau/m) , \\ \dot{z}_1 &= (n\eta/m)z_2 - \dot{\xi}\cos(n\eta\tau/m) - \dot{\zeta}\sin(n\eta\tau/m) , \\ \dot{z}_2 &= \dot{\xi}\sin(n\eta\tau/m) - \dot{\zeta}\cos(n\eta\tau/m) + (n\eta/m)(y_1 - z_1) \\ &\quad - g(y_1)y_2 - (m/n\eta)f(y_1, \tau) . \end{aligned}\right\} \quad (9)$$

Componnets z_1 and z_2 of solution (8) are not necessary for some

cases like resonances of orders 1 and 1/2 with symmetric restoring forces. Averaging the right-side hand over 0 to 2π, we obtain

$$\left.\begin{aligned}\dot{\xi} &= -(n\eta/2m)\zeta + G_s + (m/n\eta)F_s \\ \dot{\zeta} &= (n\eta/2m)\xi - G_c - (m/n\eta)F_c\end{aligned}\right\} \qquad (10.a)$$

$$\left.\begin{aligned}\dot{z}_1 &= (n\eta/m)z_2 \\ \dot{z}_2 &= -G_o - (m/n\eta)F_o\end{aligned}\right\} \qquad (10.b)$$

where

$$F_s = \frac{1}{2\pi}\int_0^{2\pi} f(y_1, \tau)\sin\left(\frac{n\eta\tau}{m}\right)d\left(\frac{n\eta\tau}{m}\right), \quad F_o = \frac{1}{2\pi}\int_0^{2\pi} f(y_1, \tau)d\left(\frac{n\eta\tau}{m}\right).$$

F_c is replaced with cos instead of sin and G_s, G_c and G_o are with $g(y_1)y_2$ instead of $f(y_1, \tau)$ (see Appendix).

In a similar way we also obtain the differential equations for A and ϕ instead of Eq.(10.a).

$$\left.\begin{aligned}\dot{A} &= \bar{G}_s + (m/n\eta)\bar{F}_s \\ \dot{\phi} &= n\eta/2m - \bar{G}_c/A - (m/n\eta A)\bar{F}_c\end{aligned}\right\} \qquad (11.a)$$

where $\dot{z}_1$ and $\dot{z}_2$ are the same as Eq.(10.b). $\bar{G}$ and $\bar{F}$ are respectively replaced with $\sin(n\eta\tau/m - \phi)$ and $\cos(n\eta\tau/m - \phi)$ instead of $\sin(n\eta\tau/m)$ and $\cos(n\eta\tau/m)$ of G and F like

$$\bar{F}_s = \frac{1}{2\pi}\int_0^{2\pi} f(y_1, \tau)\sin\left(\frac{n\eta\tau}{m} - \phi\right)d\left(\frac{n\eta\tau}{m}\right).$$

Coordinates $A - \phi$ and $\xi - \zeta$ are connected with the following relations:

$$\left.\begin{aligned}\dot{A} &= \dot{\xi}\cos\phi + \dot{\zeta}\sin\phi \\ A\dot{\phi} &= -\dot{\xi}\sin\phi + \dot{\zeta}\cos\phi\end{aligned}\right\} \qquad (12)$$

It is revealed that Eqs.(10) and (11) led by the averaging method describe the following two kinds of solutions:

(1) Resonances ($\dot{\xi} = \dot{\zeta} = \dot{z}_1 = \dot{z}_2 = 0$)

(2) Amplitude-modulated motions corresponding to limit cycles in the plane $\xi - \zeta$

But for the components z_1 and z_2, the plane $\xi - \zeta$ by the averaging method is the same as the coordinates $\xi - \zeta$ in Sec.4.1. Then it is important to examine the trajectory of Eq.(10) in the plane $\xi - \zeta$.

6. Numerical Examples and Consideration

6.1 Comparison of phase trajectories

We shall solve the following two types of systems numerically and investigate their behaviors by the phase trajectories proposed

in Chapter 4:

$$\ddot{y} - (0.05 - \delta_2 y^2)\dot{y} + f(y, \tau) = 0 \qquad (13)$$

with parameters shown in Table 4.

Table 4 Parameters of Eq.(13)

System	δ_2	$f(y, \tau)$
I	0.01	$(1 + 0.01y^2 + 0.2 \cos 2\eta\tau)y$
II	0.02	$(1 + 0.2y^2)(1 + 0.2 \cos 2\eta\tau)y$

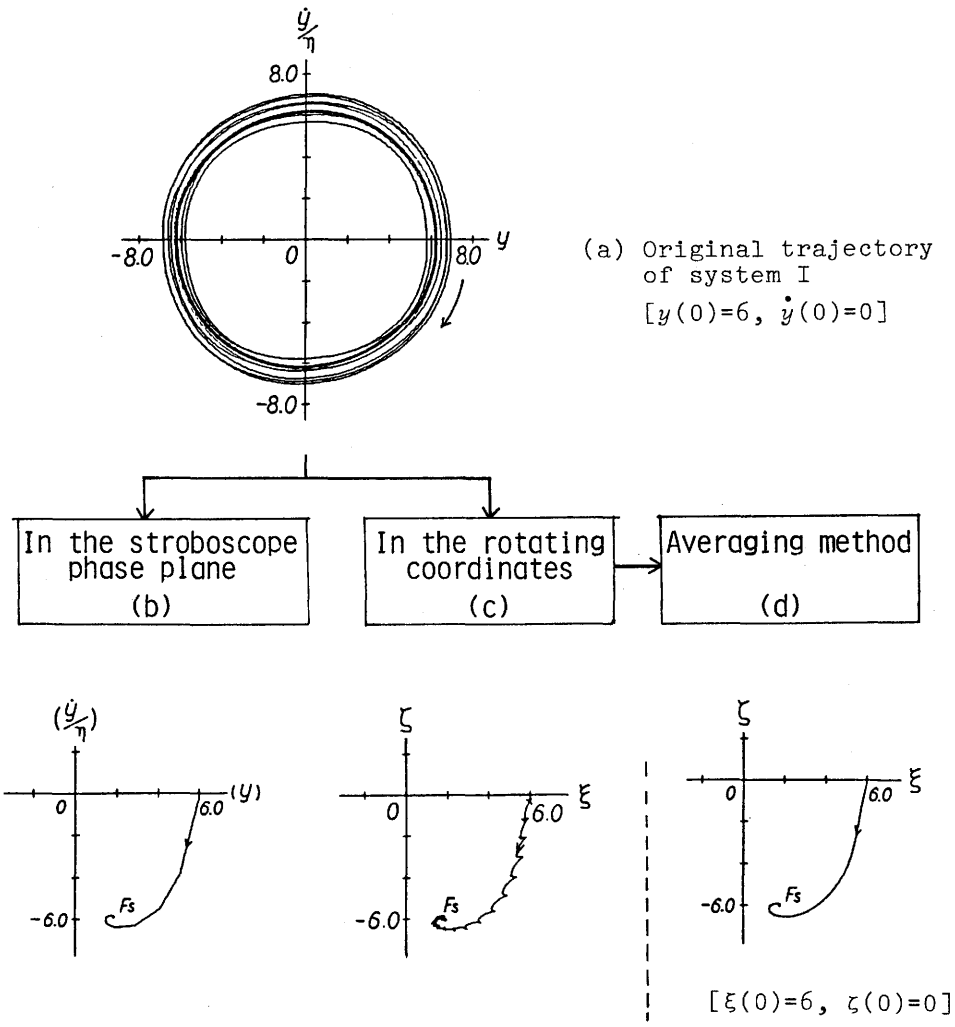

Fig.6 Expression of trajectories
(η=1.1; resonance of order 1)

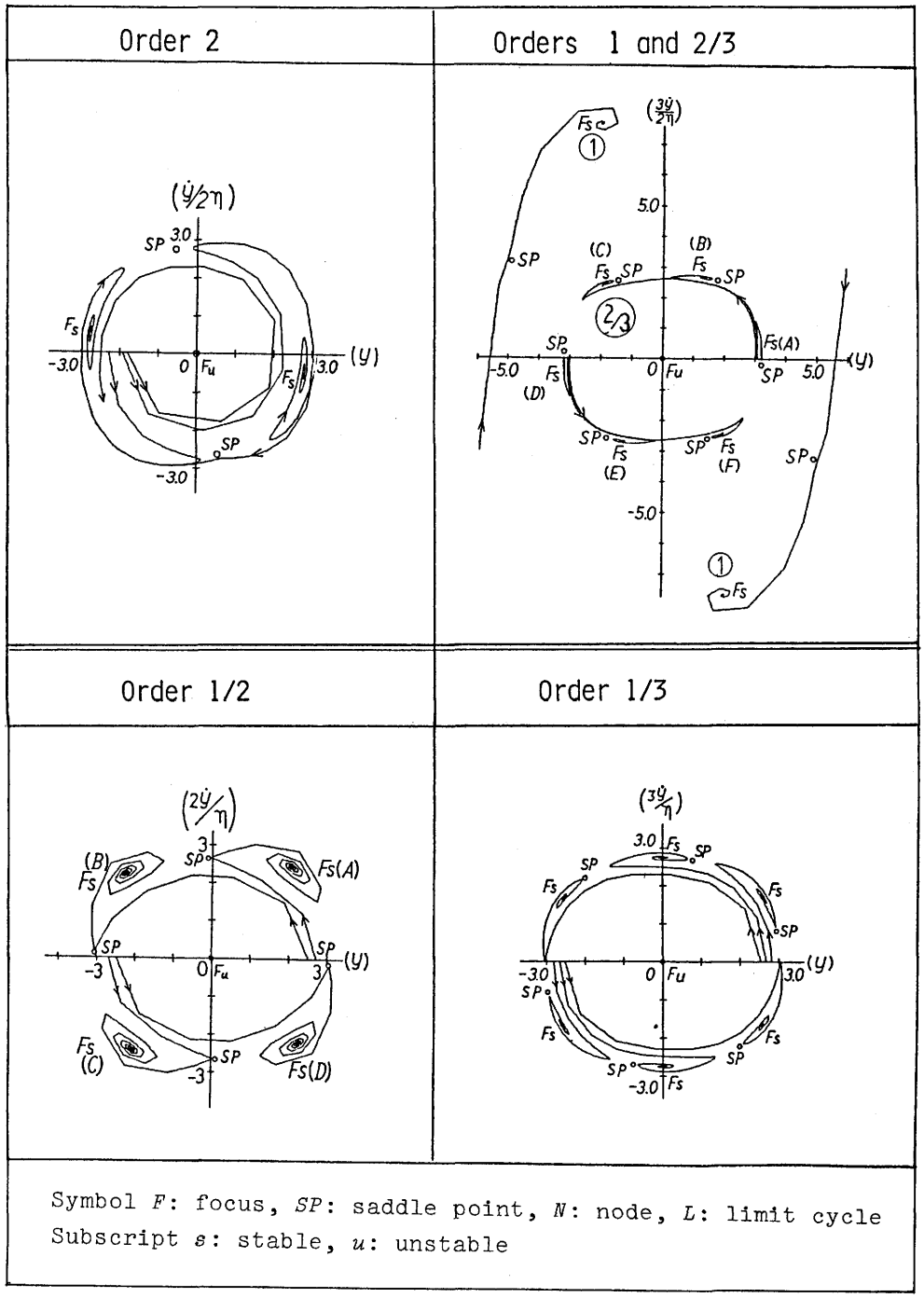

Fig.7 Resonances of system II in the stroboscope phase plane

It is well observed from Figs.6(b) and (c) that such an aspect that each trajectory of system I converges toward a resonance of order 1 marked by symbol F_S at $\eta = 1.1$ instead of an original trajectory in Fig.(a). In the stroboscope phase plane the breaking points represent reference points at every period. The trajectory of Eq.(10) by the averaging method shown in Fig.6(d) also describes that aspect plainly. Figure 7 shows main and some kinds of resonances of system II investigated in the stroboscope phase plane.

As for the behavior in the neighborhood of resonances, it is convenient to investigate it by trajectories in the rotating coordinates with an angular velocity $n\eta/m$. Figure 8 shows that a complicated original trajectory of system I can be grasped as a closed orbit like a limit cycle at the frequency just upper the resonance of order 1. At the frequency distant from the resonance, Fig.9(a) shows that a limit cycle of Eq.(10) (symbol L_S) by the averaging method indicated by a dot-dash-line corresponds to an inner envelope of original trajectory. Then the pattern of vibration of system I is shown in Fig.9(b). Points P_1, P_2, ... of waveform representing local maximum deflections actually correspond to the bottoms of curved parts of trajectory, where L_S passes. The sharp-pointed point Q_1 corresponds to the point where the deflection is zero. Accordingly it is seen that the maximum amplitude of vibration will be estimated by the maximum values of the limit cycle.

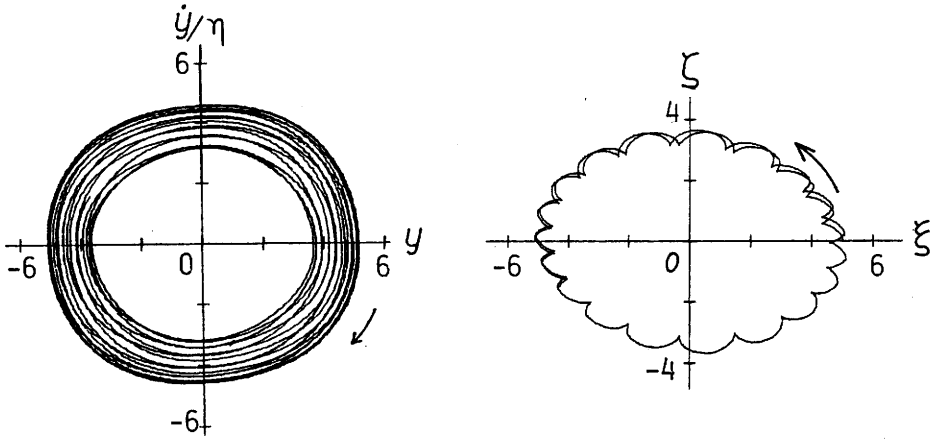

(a) Original trajectory (b) In the rotating coordinates

Fig.8 Trajectories in the neighborhood of resonance of order 1 [system I; η=1.2; $y(0)$=5, $\dot{y}(0)$=0]

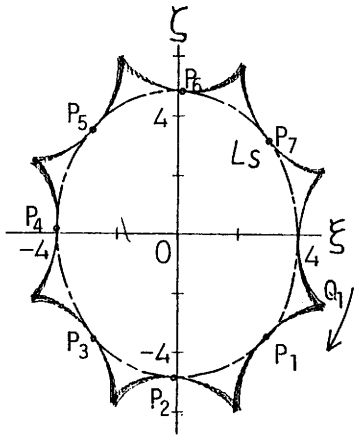

(a) Trajectory in the rotating coordinates

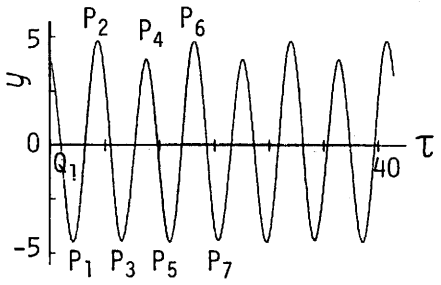

(b) Pattern of vibration

Fig.9 Relation between trajectories and waveforms [system I; $\eta=0.8$; $y(0)=4$, $\dot{y}(0)=0$]

6.2 Consideration of nonlinear models

In reference to making available nonlinear models, Table 5 shows kinds and orders of resonances occurring in systems I and II. The property of each resonance, which is evidently different from that of well-known forced nonlinear systems, is presented in Ref.(9).

It is seen that the presence of exciting term $y^k\cos 2\eta\tau$ determines the orders of resonances to be explained by nonlinear models. In systems with only the term of $k=1$, resonances of order n (n=1, 2, 3 ...), that is, only main and superharmonic resonances occur at the frequencies near $\eta = 1/n$ even if the nonlinear term y^k of higher orders ($k \geqq 4$) is included in the restoring force. That fact is supplemented by the following Mathieu equation with only nonlinear damping:

$$\ddot{y} + 0.01y^2\dot{y} + (1 + 0.2\cos 2\eta\tau)y = 0 \qquad (14)$$

Table 5 Orders of resonances

Systems with $y^k\cos 2\eta\tau$	Orders of resonances			
	Super-	Main	Sub-	Subsuper-
k=1	2	1		
k=3 (k=1 and 3)	2	1	1/2, 1/3	2/3

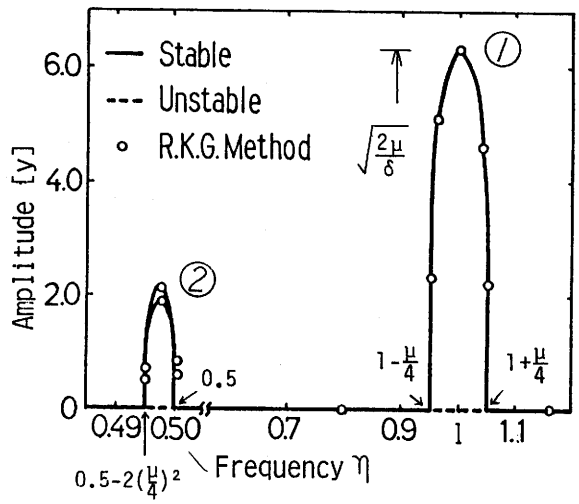

Fig.10 Resonance curves of Eq.(14) without self-excitation

and the results of approximate analyses shown in Fig.10, where the boundaries of instability of solutions predicted from linear models are also indicated.

In the case of cracked rotors, though the external excitation by unbalance force also works, the kind of resonances occurring might be predicted from systems with the exciting term of k=1 (see Fig.1). As for resonances of such higher orders as shown in Fig.2 and Table 1, it is necessary to investigate which resonances are interpreted by which exciting terms. The exciting term of k=2 will be unimportant in essence.

7. Concluding Remarks

In order to investigate the behaviors of rotors with a crack, a rub and the looseness, some nonlinear models are described mathematically and are solved numerically. Vibrational phenomena explained by their models are examined through trajectories expressed in the rotating coordinates and in the stroboscope phase plane. As for resonances of one-degree-of-freedom systems, their occurrence besides a main resonance (order 1) is considered as follows:

For $\eta < 1$: Resonances of order n at $\eta \simeq 1/n$

For $\eta > 1$: Resonances of order n/m at $\eta \simeq m/n$

Hereafter it is required to construct more available models of actual phenomena.

Acknowledgement

The author heartily thanks Dr. A. Muszynska, Senior Research Scientist of Bently Rotor Dynamics Research Corporation, for his presentation of many papers on the instability in rotating machinery.

References

(1) Childs, D.W.: Trans.ASME, J. Engineering for Power, 104 (1982), pp.533-541.

(2) Schmied, J. and Krämer, E.: Vibrations in Rotating Machinery, IMechE (1984), pp.183-192.

(3) Muszynska, A.: Shaft Crack Detection, Seventh Machinery Dynamics Seminar (1982), National Research Council Canada.

(4) Muszynska, A.: Synchronus and Self-excited Rotor Vibrations Caused by a Full Annular Rub, Eighth Machinery Dynamics Seminar (1984), ibid.

(5) Grissom, B.: Partial Rotor to Stator Rub Demonstration, Exhibit "Instability in Rotating Machinery" (1985), Bently Nevada Corpration.

(6) Muszynska, A.: Rotor Instability Due to Loose Rotating Part, ibid.

(7) Parks, P.C. and Tondl, A.: Proc. 8th International Conference on Nonlinear Oscillations (1978), pp.69-86.

(8) Tondl, A.: Monographs and Memoranda No.25 (1978), National Research Institute for Machine Design, Běchovice.

(9) Yano, S.: Basic Studies on Parametric Vibrations (in Japanese), Dissertation of Kyoto University (1984).

Appendix

F, G, $\bar{F}$ and $\bar{G}$ of Eqs.(10) and (11) are presented in Tables 6 and 7 when $\delta_0=\beta$ and $\delta_2=\delta$ for type 1 and $\gamma_3=\gamma$, $\gamma_2=0$, $s=3$ in Table 2.

Table 6 F and G of Eq.(10)

Order	Type	G_s	G_c	F_s	F_c
1	1	$G_{11}\xi$	$-G_{11}\zeta$	$(F_{11}-\frac{\mu}{2})\frac{\zeta}{2}$	$(F_{11}+\frac{\mu}{2})\frac{\xi}{2}$
	2			$\{F_{11}-\frac{\mu}{2}(1+\gamma\zeta^2)\}\frac{\zeta}{2}$	$\{F_{11}+\frac{\mu}{2}(1+\gamma\xi^2)\}\frac{\xi}{2}$
1/2	2			$\{F_{11}-\frac{\mu\gamma}{8}(3\xi^2-\zeta^2)\}\frac{\zeta}{2}$	$\{F_{11}+\frac{\mu\gamma}{8}(\xi^2-3\zeta^2)\}\frac{\xi}{2}$

Table 6 (continued)

Order	Type	G_s	G_c	F_s	F_c
2	1	$G_{12}\xi+\delta\zeta z_1 z_2$	$-G_{12}\zeta+\delta\xi z_1 z_2$	$F_{12}\frac{\zeta}{2}$	$F_{12}\frac{\xi}{2}+\frac{\mu}{2}z_1$
	2			$F_{12}\frac{\zeta}{2}+\frac{3\mu\gamma}{4}\xi\zeta z_1$	$F_{12}\frac{\xi}{2}+\frac{\mu z_1}{2}\{1+\frac{3\gamma}{4}(3\xi^2+\zeta^2)+\gamma z_1^2\}$

G_o	F_o
$-\{\beta-\frac{\delta}{2}(A^2+2z_1^2)\}z_2$	$F_{13}z_1+\frac{\mu}{2}\xi$
	$F_{13}z_1+\frac{\mu}{2}F_{12}\xi$

G_{11}	G_{12}	F_{11}	F_{12}	F_{13}
$\frac{1}{2}(\beta-\frac{\delta}{4}A^2)$	$\frac{1}{2}\{\beta-\frac{\delta}{4}(A^2+4z_1^2)\}$	$1+\frac{3\gamma}{4}A^2$	$1+\frac{3\gamma}{4}(A^2+4z_1^2)$	$1+\frac{3\gamma}{2}(A^2+\frac{2}{3}z_1^2)$

Table 7 $\bar{F}$ and $\bar{G}$ of Eq.(11)

Order	Type	$\bar{G}_s$	$\bar{F}_s$	$\bar{F}_c$
1	1	$G_{11}A$	$-\frac{\mu A}{4}\sin 2\phi$	$(F_{11}+\frac{\mu}{2}\cos 2\phi)\frac{A}{2}$
	2		$-\frac{\mu A}{8}(2+\gamma A^2)\sin 2\phi$	$\{F_{11}+\frac{\mu}{2}(1+\gamma A^2)\cos 2\phi\}\frac{A}{2}$
1/2	2		$-\frac{\mu\gamma}{16}A^3\sin 4\phi$	$(F_{11}+\frac{\mu\gamma}{8}A^2\cos 4\phi)\frac{A}{2}$
2 *	1		$-\frac{\mu z_1}{2}\sin\phi$	$(F_{11}+\frac{\mu z_1}{A}\cos\phi)\frac{A}{2}$
	2		$-\frac{\mu z_1}{2}(1+\frac{3\gamma}{4}A^2)\sin\phi$	$\{F_{11}+\frac{\mu z_1}{A}(1+\frac{9\gamma}{4}A^2\cos\phi\}\frac{A}{2}$

$\bar{G}_c=0$ * On the assumption that $A^2 \gg z_1^2$

$\bar{G}_s=\frac{1}{2\pi}\int_0^{2\pi} g(y_1)y_2\sin(\frac{n\eta\tau}{m}-\phi)d(\frac{n\eta\tau}{m})$

For $g(y)$ of type 2 in Table 2, $G_{11}=-\frac{1}{2}(\delta_0-\frac{\delta_2}{4}A^2+\frac{\delta_4}{8}A^4)$ holds in G_s and $\bar{G}_s$. Furthermore when $g(y)\dot{y}=\kappa\,\mathrm{sgn}\,\dot{y}$ is also included together with self-excitation of type 1, each β in G_{11}, G_{12} and $\bar{G}_s$ is replaced with $\beta-\frac{4\kappa}{\pi A}(\frac{m}{n\eta})$.

As for the stability analysis of approximate solutions, the following characteristic equation derived from Eq.(10) by introducing small variations into steady state solutions provides stability conditions:

$$\begin{vmatrix} a_{11}-\lambda & a_{12} \\ a_{21} & a_{22}-\lambda \end{vmatrix}$$

$$= \lambda^2-(a_{11}+a_{22})\lambda + a_{11}a_{22}-a_{12}a_{21} = 0 \qquad (A.1)$$

where a_{ij} $(i, j = 1, 2)$ are shown in Table 8 for resonances of order $1/m$ $(m=1, 2)$ of systems with symmetric restoring forces. The subscript s denotes steady state solutions.

Table 8 a_{ij} of Eq.(A.1)

a_{11}	$P_0P_2 + \bar{S}_1/2$
a_{12}	$(m/2\eta)\{P_1-(\mu/2)P_3+(3\gamma/2)P_4\zeta_s^2\} + \bar{S}_2/4$
a_{21}	$-(m/2\eta)\{P_1+(\mu/2)P_3+(3\gamma/2)P_5\xi_s^2\} + \bar{S}_2/4$
a_{22}	$-P_0P_2 + \bar{S}_3/2$
$P_0=(3\gamma/8\eta)A_s^2\sin 2\phi_s$, $P_1=1+3\gamma A_s^2/4-(\eta/m)^2$	

Order	type	P_2	P_3	P_4	P_5
1	1	1			
	2	1		$1-\mu$	$1+\mu$
1/2	2	$2-\mu$	$(3\gamma/4)A_s^2\cos 2\phi_s$	1	

$\bar{S}_i$ $(i=1, 2, 3)$ are determined in accordance with the type of self-excitation. For example, for type 2 in Table 2, those are as follows:

$$\bar{S}_1 = -S_0+S_1\xi_s^2 , \quad \bar{S}_2 = S_1A_s^2\sin 2\phi_s , \quad \bar{S}_3 = -S_0 + S_1\zeta_s^2$$

where

$$S_0 = \delta_0-\delta_2A_s^2/4+\delta_4A_s^2/8, \quad S_1 = (\delta_2-\delta_4A_s^2)/2.$$